Pergamon

Int. J. Multiphase Flow Vol. 22, No. 2, pp. 353–361, 1996

0301-9322(95)00074-7
0301-9322/96 $15.00 + 0.00

A NEW CRITERION FOR THE CONTINUOUS OPERATION OF SUPERSETTLERS IN THE BOTTOM FEEDING MODE

A. TRIPATHI and A. ACRIVOS
The Benjamin Levich Institute, The City College of the City University of New York, New York, NY 10031, U.S.A.

(Received 19 July 1995; in revised form 7 November 1995)

Abstract—By considering the hydrodynamic interaction between the suspension and the concentrated sediment in an inclined settler operation continuously in the bottom feeding mode, a new upper bound is derived for the maximum value of the volumetric feed rate which can be tolerated under a given set of conditions. This criterion is distinct from the familiar Ponder–Nakamura–Kuroda formula which results from applying simple kinematic arguments.

Key Words: inclined settler, sedimentation, supersettlers

1. INTRODUCTION

Consider a typical supersettler, sketched in figure 1, being operated continuously in the bottom feeding mode. We suppose that the feed consists of a well mixed monodisperse suspension of heavy spherical particles. As the suspension flows inside the settler under conditions where the particle Reynolds number is vanishingly small, the particles slip in the direction of gravity relative to the liquid and then form a concentrated sediment upon reaching the upper-facing surface of the settler. As a result, the interior of the settler contains three distinct fluid phases: (1) a particle free layer underneath the downward facing surface; (2) the bulk of the suspension where the particle volume fraction ϕ_s equals that in the feed; and (3) the sediment layer referred to above. It follows that, if the settler is long enough, all the particles will sediment out of the suspension and that the overhead product will consist only of pure liquid. Clearly, such a continuous operation is possible only if the sediment can flow freely under gravity along the upward facing wall so that the particles can be collected at the bottom of the settler and be removed.

Let Q_{s0} and Q_{d0} denote, respectively, the volumetric flow rates, per unit depth, of the feed and that of the sediment at the bottom of the settler and let us suppose further that the particle volume fraction within the sediment equals the given value ϕ_d. Then, provided the overhead product is devoid of particles, we have, on account of an overall particle balance around the settler, that

$$Q_{s,0}\,\phi_s - Q_{d,0}\,\phi_d = 0. \qquad [1]$$

In addition, let us suppose that the sediment along the upward facing surface extends over a distance L^* from the bottom of the settler, and let $u_t f(\phi_s)$ denote the settling speed of a representative particle within the suspension, where u_t refers to the Stokes settling speed of an isolated sphere and $f(\phi_s)$ is the familiar settling hindrance function which, following the usual practice, is taken to depend only on ϕ_s. A second overall particle balance around the sediment layer then yields

$$Q_{d0}\,\phi_d = Q_{d0}\,\phi_s + L^*\phi_s\,u_t\,f(\phi_s)\cos\theta \qquad [2]$$

and hence, on account of [1],

$$Q_{s0} = \frac{L^* u_t\,f(\phi_s)\cos\theta}{(1-\phi_s/\phi_d)} \qquad [3]$$

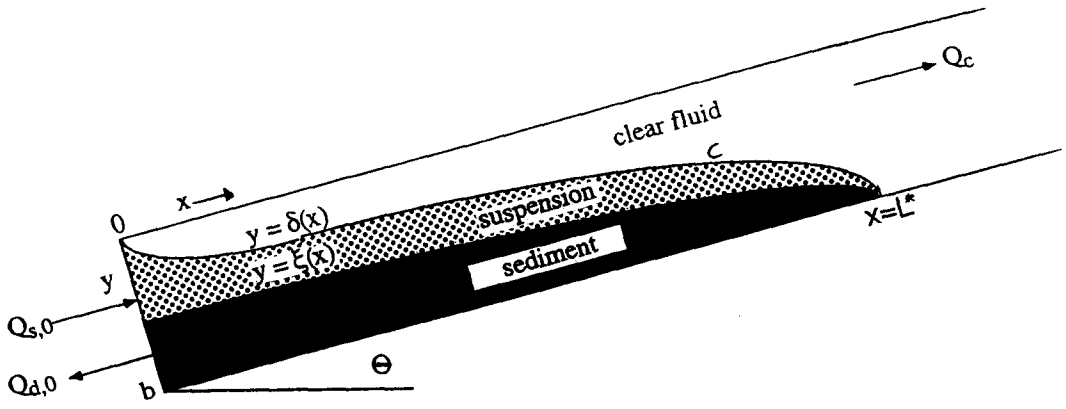

Figure 1. View of the inclined settler showing the definitions of the variables used in the analysis.

which relates Q_{s0} and L^*. In particular, in a settler of given length L, the volumetric feed rate Q_{s0} cannot exceed

$$Q_{s0}(\max) = \frac{Lu_t(\phi_s)\cos\theta}{(1-\phi_s/\phi_d)} \qquad [4]$$

if the overhead product is to remain free of particles. This is well known Ponder–Nakamura–Kuroda (PNK) formula (see Acrivos & Herbolzheimer 1979), modified to account for the presence of a sediment layer, which has played a key role in the design of supersettlers.

The expression given above for the maximum volumetric feed rate presupposes that the interface between the clear fluid and the suspension—c.f. curve C in figure 1—remains stable and that any waves which may be generated do not break and thereby entrain particles into the clarified liquid. The stability of the flow configuration within supersettlers has therefore been studied extensively both theoretically as well as experimentally by Davis *et al.* (1983) and by Leung & Probstein (1983). On the other hand, as was mentioned earlier, another condition for the continuous operation of supersettlers, and therefore of the applicability of the PNK formula, refers to the requirement that the sediment layer be able to flow under gravity, so that the particles which have already settled can be removed. As we shall see presently, for a certain range of parameters, this can lead to values of the maximum permissible volumetric feed rate $Q_{s0}(\max)$ which fall below those given by the PNK formula [4].

In two recent articles by Nir & Acrivos (1990) and by Kapoor & Acrivos (1995), the flow of a sediment layer that forms on an inclined plate in contact with a suspension of sedimenting particles above it, was investigated by means of a model in which the downward gravitational particle flux is opposed by a shear-induced particle flux due to gradients in the particle concentration and in the shear stress. In general, as a consequence of this balance, the particle concentration within the sediment will remain everywhere below its maximum value $\phi_m \sim 0.58$, at which the suspension viscosity becomes infinite, and hence the sediment is able to flow under the action of gravity. It was also shown, however, that, if the angle of inclination θ falls below a critical value approximately equal to 10° for a wide range of ϕ_s, a steady operation is no longer feasible and that the thickness of the sediment layer will grow indefinitely with time. This results from the fact that, at a critical angle, the particle concentration in the sediment adjacent to the upward facing surface equals the maximum value ϕ_m and, therefore, that portion of the sediment, on account of its infinitely large viscosity, is unable to flow and remains attached to the plate (see Kapoor & Acrivos 1995).

This analysis referred to above was, however, restricted to "low" aspect ratio settlers in which both the sediment and the clear fluid layers are everywhere very thin compared to the spacing, b, between the plates. But, from a practical point of view, one is primarily interested in the operation of "high" aspect ratio settlers, in which the thickness of the sediment and that of the clear fluid layer are comparable to b, because such settlers offer both increased efficiency as well as stability (see Davis *et al.* 1983). The flow of the suspension within a "high" aspect ratio vessel is accompanied, however, by a pressure drop along its length which opposes the downward flow of

the sediment, and hence, even if the conditions for the sediment flow set forth earlier by Kapoor & Acrivos (1995) are satisfied, i.e. even if the particle volume fraction adjacent to the upward facing surface remains below ϕ_m, the increased pressure drop resulting from an increase in Q_{s0} will eventually prevent the sediment from reaching the bottom of the settler and be collected. This then places a restriction on the maximum value of Q_{s0} which is quite distinct from that given by [4]. It is the purpose of this paper to derive an expression for this upper bound on Q_{s0} which does not appear to have been given before.

2. THEORETICAL ANALYSIS

Following Probstein *et al.* (1981) and Leung & Probstein (1983), we suppose that the settler is long enough relative to its width, so that the flow within each of the three phases, referred to earlier and depicted in figure 1, is everywhere quasi-parallel.† In addition, we model the suspension and the sediment as effective Newtonian fluids having viscosities, relative to that of the clear liquid, equal to $\lambda(\phi_s)$ and $\lambda(\phi_d)$, respectively, where ϕ_s and ϕ_d are the corresponding particle volume fractions. Also, since it has been shown recently that, within a sediment flowing along the inclined plate, the particle concentration is, in general, fairly uniform, we shall take ϕ_d to be a constant and shall estimate its value by referring to the results of the more elaborate calculations presented by Kapoor & Acrivos (1995).

Under these circumstances then, the dimensionless Navier–Stokes equations within the clear fluid layer $0 < y < \delta(x)$ reduce to

$$\frac{\partial^2 u}{\partial y^2} - \frac{dP}{dx} + \Gamma \sin\theta = 0 \qquad [5]$$

where u is the longitudinal component of the bulk velocity rendered dimensionless with u_t, y and x are, respectively, the transverse and longitudinal coordinates rendered dimensionless with b, the spacing between the plates and P is the dynamic pressure divided by $u_t \mu_f / b$ where μ_f refers to the pure fluid viscosity. Finally

$$\Gamma = \frac{b^2 g\, \Delta\rho}{u_t \mu_f} \phi_s = \frac{9}{2}\left(\frac{b}{a}\right)^2 \phi_s \qquad [6]$$

where a is the radius of one of the spherical particles, g is the gravitational constant and $\Delta\rho$ is the difference between the density of the solid particles and that of the fluid. Similarly, within $\delta(x) < y < \xi(x)$ the region occupied by the suspension, we have

$$\lambda(\phi_s)\frac{\partial^2 u}{\partial y^2} - \frac{dP}{dx} = 0 \qquad [7]$$

while, within the sediment, $\xi(x) < y < 1$,

$$\lambda(\phi_d)\frac{\partial^2 u}{\partial y^2} - \frac{dP}{dx} + \Gamma\left(1 - \frac{\phi_d}{\phi_s}\right)\sin\theta = 0. \qquad [8]$$

Equations [5], [7] and [8], subject to the boundary conditions of no-slip at the two walls plus the requirement that the velocity and the shear stress be continuous across each of the two interfaces, can be readily integrated to yield the corresponding expressions for the velocities which are given in the appendix. Using these velocity profiles, we obtain the following expressions for the volumetric flow rates per unit depth, rendered dimensionless with bu_t,

$$Q_c \equiv \int_0^{\delta(x)} u\, dy = F_3 \frac{dP}{dx} + F_4 \Gamma \sin\theta \qquad [9]$$

†This quasi-parallel assumption does not apply of course near $x = 0$ and $x = L^*/b$, i.e. within the entry and exist regions where inertia effects play an important role. For moderate values of the bulk Reynolds number, however, the lengths of these regions are comparable to b, and hence their influence can be neglected in "high" aspect ratio vessels for which $L^*/b \gg 1$.

$$Q_s \equiv \int_{\delta(x)}^{\xi(x)} u \, dy = F_5 \frac{dP}{dx} + F_6 \Gamma \sin\theta \qquad [10]$$

$$Q_d \equiv -\int_{\xi(x)}^{1} u \, dy = -F_7 \frac{dP}{dx} - F_8 \Gamma \sin\theta \qquad [11]$$

where the Fs are functions of $\delta(x)$, $\xi(x)$, ϕ_s and ϕ_d as given in the appendix. We note that, if $\lambda(\phi_s)$ is set equal to unity, [9]–[11] become identical to those derived by Leung & Probstein (1983).

Next, to determine the remaining unknowns, $\delta(x)$, $\xi(x)$ and dP/dx, we make use of the requirement that the particle flux be continuous across each of the two interfaces, $y = \delta(x)$ and $y = \xi(x)$, and that the net volumetric flow rate $Q_{net} \equiv Q_c + Q_s - Q_d$ be independent of x. These conditions lead to, respectively,

$$\frac{dQ_c}{dx} = f(\phi_s)\cos\theta, \quad \frac{dQ_s}{dx} = -\frac{\phi_d f(\phi_s)\cos\theta}{(\phi_d - \phi_s)} \quad \text{and} \quad \frac{dQ_d}{dx} = -\frac{\phi_s f(\phi_s)\cos\theta}{(\phi_d - \phi_s)}. \qquad [12]$$

On integrating these along the length of the settler, we obtain that

$$Q_c = xf(\phi_s)\cos\theta, \quad Q_s = Q_{s,0} - \frac{x\phi_d f(\phi_s)\cos\theta}{(\phi_d - \phi_s)} \quad \text{and} \quad Q_d = \frac{\phi_s}{\phi_d} Q_s, \qquad [13]$$

where on account of [1], we have set $Q_{d,0} = Q_{s0}\phi_s\phi_d$. Note that [13] differs from [34]–[36] in Leung & Probstein (1983), who used an incorrect expression for the continuity of particle flux across the interface $y = \xi(x)$. Finally, on using the fact that both $Q_s(x)$ and $Q_d(x)$, as given by [13], must vanish at $x = L^*/b$, we recover the expression for $Q_{s,0}$ given by [3], if the latter is rendered dimensionless by dividing both sides with bu_t. Thus, for a given dimensionless inlet feed rate $Q_{s,0}$, we have that, as before

$$\frac{L^*}{b} = \frac{Q_{s,0}(\phi_d - \phi_s)}{\phi_d f(\phi_s)\cos\theta}. \qquad [14]$$

As was said earlier, for a settler of finite length L, a necessary condition for the present analysis to apply is that $L^* \leqslant L$, because, if the feed rate exceeds the maximum value given by [4], the excess suspension will leave the settler together with the clear fluid.

In addition, however, we require that [9]–[14] have a solution with $\delta = 0$ at $x = 0$ and $\xi = 1$ at $x = L^*/b$. We therefore examine the set, which we obtain by substituting the corresponding flow rates from [13] into [9]–[11],

$$-F_3 F + \beta F_4 = \frac{bx}{L^*} \qquad [15]$$

$$-F_5 F + \beta F_6 = \frac{\phi_d}{(\phi_d - \phi_s)}\left(1 - \frac{bx}{L^*}\right) \qquad [16]$$

$$-F_7 F + \beta F_8 = \frac{\phi_s}{(\phi_d - \phi_s)}\left(\frac{bx}{L^*} - 1\right) \qquad [17]$$

where F and β are given by, respectively,

$$F \equiv -\frac{\phi_d}{Q_{s,0}(\phi_d - \phi_s)} \frac{dP}{dx} = \frac{\beta(F_4 + F_6 + F_8) - 1}{F_3 + F_5 + F_7} \qquad [18]$$

$$\beta \equiv \Gamma \frac{\phi_d \sin\theta}{Q_{s,0}(\phi_d - \phi_s)}. \qquad [19]$$

Note that the relation between F and the other Fs given by [18] follows by adding [15]–[17], hence only two of the latter three equations are independent.

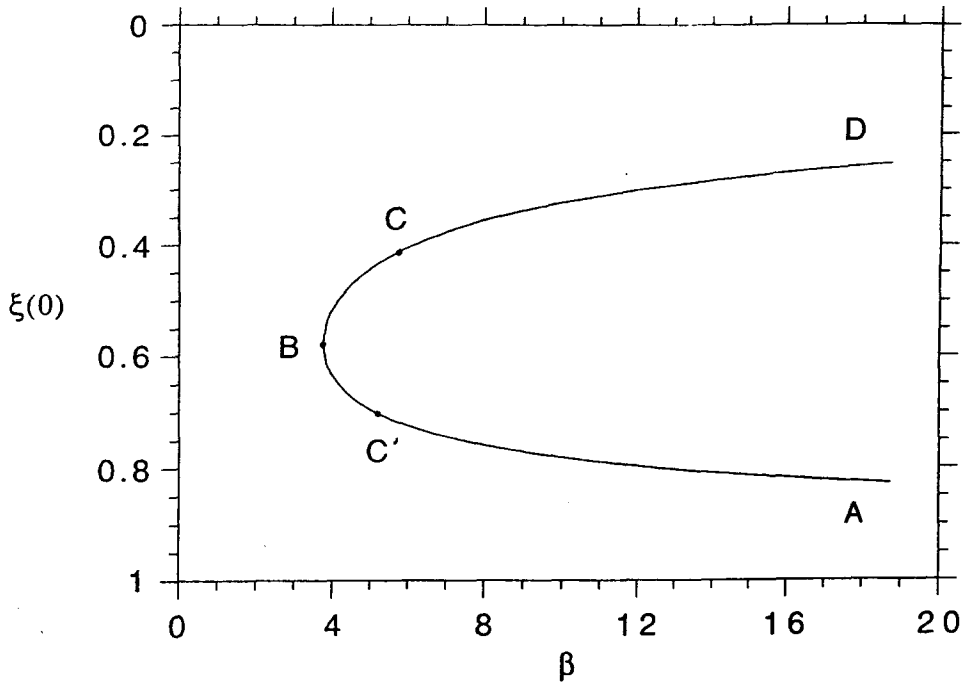

Figure 2. $\xi(0)$ as a function of β for $\phi_s = 0.01$ and $\phi_d = 0.52$.

Now, given ϕ_s, ϕ_d and β, it is a straightforward matter to determine δ and ξ, as functions of bx/L^*, by solving the set of non-linear algebraic equations [16], [17] and [18], or [15], [16] and [18], subject to the constraints: $\delta = 0$ at $x = 0$ and $\xi = 1$ at $bx/L^* = 1$. The solution can begin, of course, at either $x = 0$ or at $x = L^*/b$. In addition, we require that, at $x = 0$, the velocity u within the sediment be negative or zero everywhere which means, in particular, that $u_{s\text{-}d}$, the velocity along the suspension–sediment interface, cannot be positive at the entrance of the channel.

Now, on setting $x = 0$ and $\delta = 0$, we find that [15] is satisfied automatically and that, for a wide range of β, the remaining set of equations yields two roots for $\xi(0)$, both lying between 0 and 1, as shown in figure 2 for a typical choice of ϕ_s and ϕ_d. But, since $(d\xi/dx)_{x=0} < 0$ for any computation starting from any point along the curve BD shown in figure 2, the constraint $\xi = 1$ at $bx/L^* = 1$ cannot be satisfied using the value of $\xi(0)$ at that point as an initial condition. Also, the velocity along the suspension–sediment interface, $u_{s\text{-}d}$, is positive along the curve CD where C denotes the location of the point where $u_{s\text{-}d} = 0$. It is found moreover that, as ϕ_s decreases, C approaches point B where $(d\xi/dx)_{x=0} = 0$, and eventually crosses over to the lower branch BA (shown in figure 2 as C′) when ϕ_s falls below 0.0017 (for $\phi_d = 0.52$). Hence, as $\phi_s \to 0$, only the lower curve C′A is of any significance. We conclude therefore that the system of equations together with the constraints, as given above, has a unique solution. This was also pointed out by Leung & Probstein (1983). In addition, β cannot fall below a minimum value β_{min} given by the point B (or C′ if $\phi_s < 0.0017$ for $\phi_d = 0.52$) in figure 2. This can also be demonstrated by starting the computations at $bx/L^* = 1$ and $\xi = 1$ and then decreasing x.

At high values of β, corresponding to low feed flow rates $Q_{s,0}$, the thicknesses of both the clear fluid layer and that of the sediment are small relative to the spacing between the plates and, hence, the device operates as a "low aspect ratio" settler. But with decreasing β, i.e. with an increase in the feed flow rate $Q_{s,0}$ and therefore in the amount of material that enters the settler as feed, there is an increase in the thickness of the sediment layer at $x = 0$, as well as a corresponding increase in the pressure drop along the channel which opposes the downward flow of the sediment. This tendency of the flow to choke is illustrated in figures 3 and 4 for a typical choice of ϕ_s and ϕ_d. Moreover since, as shown in figure 2, there exists no solution for $\beta < \beta_{min}$, this places a restriction on the maximum permissible value of $Q_{s,0}$. The existence of β_{min}, whose value depends only on ϕ_s and ϕ_d, appears to have been overlooked in the earlier investigation by Leung & Probstein (1983).

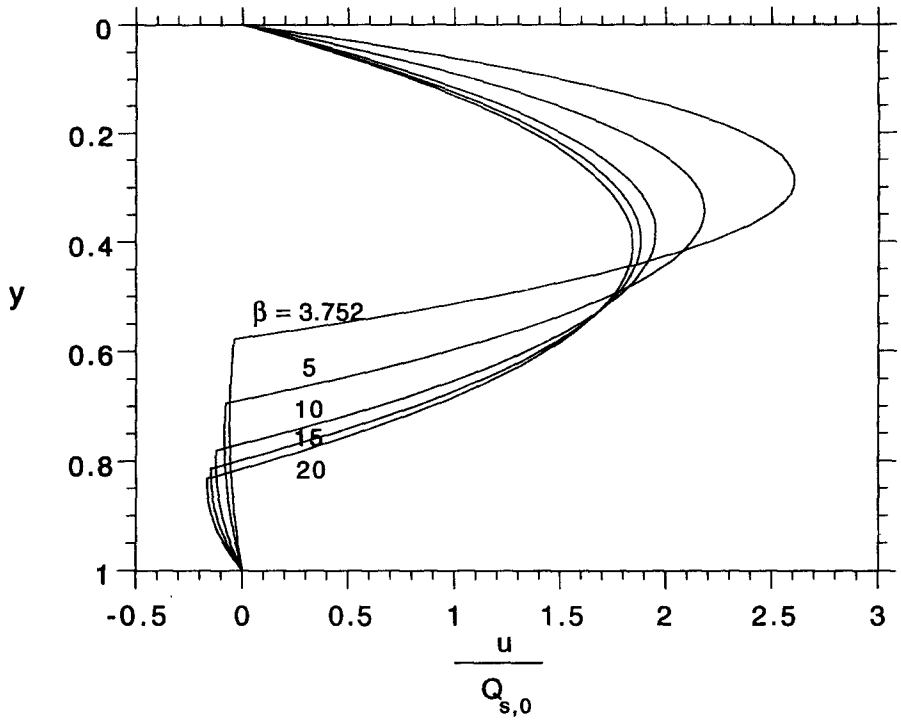

Figure 3. Dimensionless velocity profiles, $u_s(y)$ and $u_d(y)$, at $x = 0$ for $\phi_s = 0.01$ and $\phi_d = 0.52$.

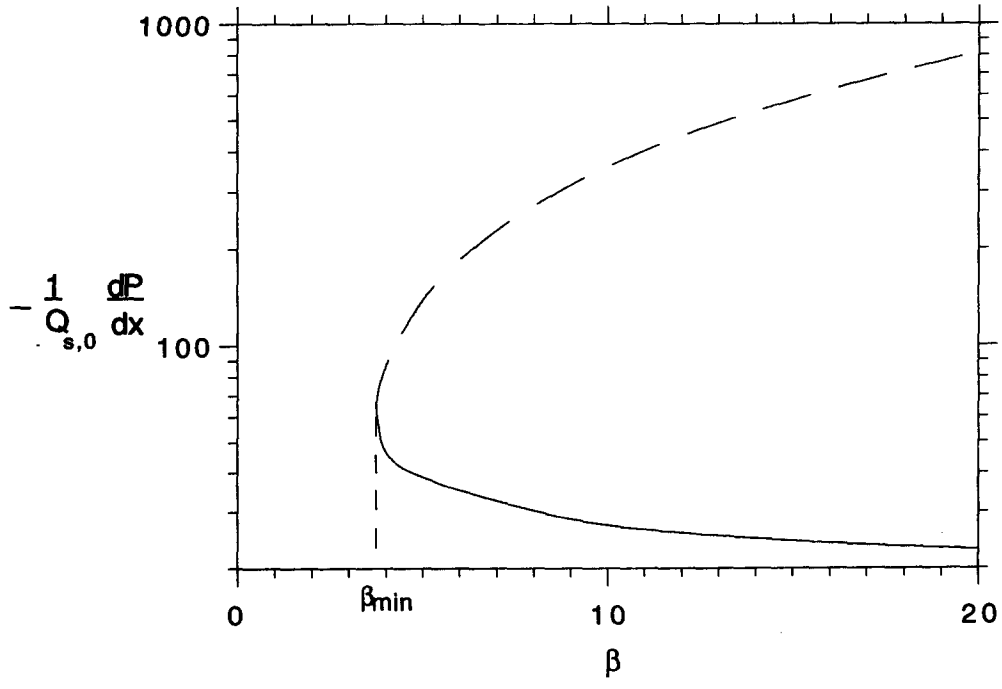

Figure 4. The dimensionless pressure gradient at $x = 0$ divided by the dimensionless feed rate, $Q_{s,0}$, as a function of β for $\phi_s = 0.01$ and $\phi_d = 0.52$ for which $\beta_{min} = 3.75$.

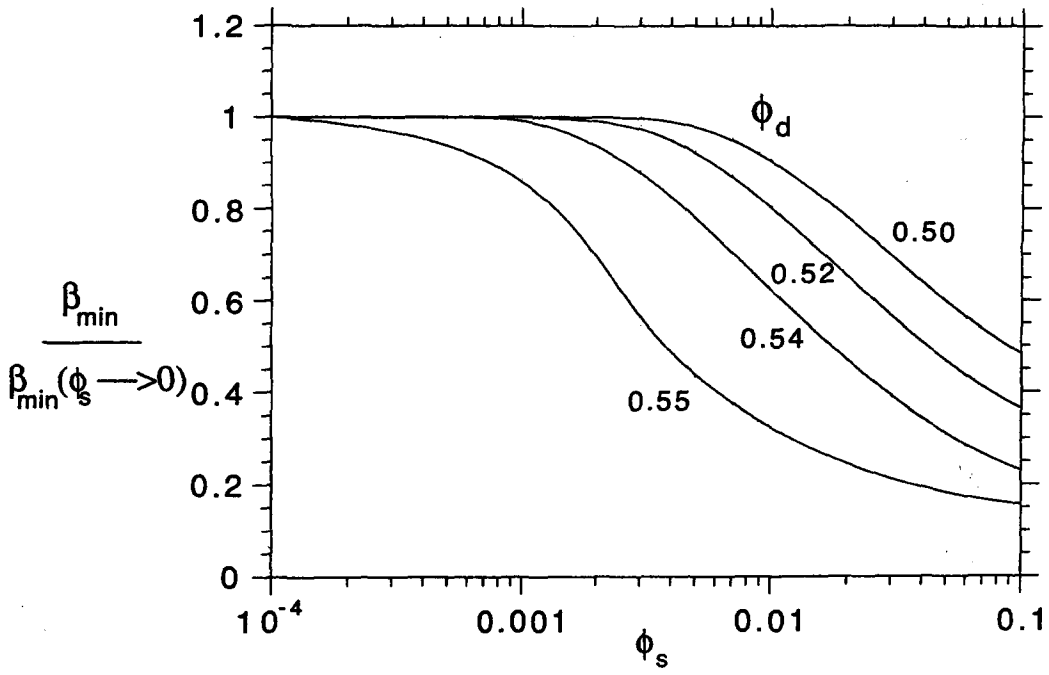

Figure 5. Numerically determined $\beta_{min}/\beta_{min}(\phi_s \rightarrow 0)$ as a function of ϕ_s with ϕ_d as a parameter. Here $\beta_{min}(\phi_s \rightarrow 0)$ is given by [20].

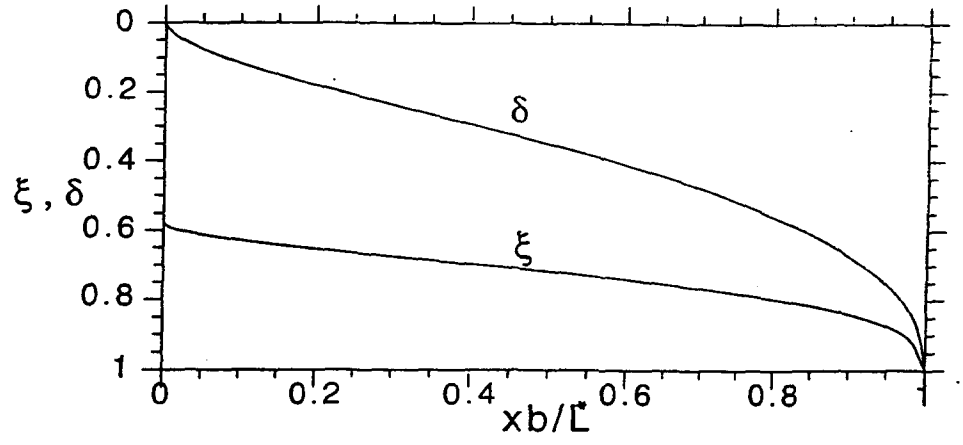

Figure 6. Profiles of $\delta(x)$ and $\xi(x)$ for $\phi_s = 0.01$, $\phi_d = 0.52$ and $\beta = \beta_{min} = 3.75$.

As was mentioned earlier, β_{min} is given by point C′ in figure 2 for $\phi_s < 0.0017$ (when $\phi_d = 0.52$). But, on noting that $u_{s-d} = 0$ at C′, we can construct the asymptotic solution of [16] and [18] at $x = 0$, as $\phi_s \rightarrow 0$, and show after some algebra that

$$\beta_{min}(\phi_s \rightarrow 0) = 12\left[1 + \sqrt{\frac{\phi_s \lambda(\phi_d)}{\phi_d}}\right]^4 \sqrt{\frac{\phi_s}{\phi_d \lambda(\phi_d)}}. \qquad [20]$$

Numerical results were obtained for β_{min}, given by the condition $(d\xi/dx)_{x=0} = 0$ (point B in figure 2) or $u_{s-d} = 0$ for $\phi_s \rightarrow 0$ (point C′). These are presented in figure 5 where we have plotted $\beta_{min}/\beta_{min}(\phi_s \rightarrow 0)$ vs ϕ_s with ϕ_d as a parameter, while, shown in figure 6, are the profiles for $\delta(x)$ and $\xi(x)$ for $\phi_s = 0.01$, $\phi_d = 0.52$ and $\beta = \beta_{min} = 3.75$. Clearly, β_{min} is a sensitive function of ϕ_d. For example, when ϕ_d is increased from 0.50 to 0.55, β_{min} increases from 3.38 to 5.68 (for $\phi_s = 0.01$).

Returning now to the conditions for determining the maximum volumetric feed rate for given values of ϕ_s and ϕ_d, we see from [14] and [19] that the dimensional flow rate $Q_{s,0}$ cannot exceed that given either by [4] or by

$$\frac{bu_t\Gamma\sin\theta}{\beta_{\min}(\phi_d,\phi_s)(1-\phi_s/\phi_d)} \qquad [21]$$

whichever is smaller. This means that $Q_{s,0}(\max)$ is given by the PNK formula, [4], for $\theta_{crit} \leqslant \theta < \pi/2$, while, for $0 < \theta \leqslant \theta_{crit}$, it equals [21], where

$$\theta_{crit} = \tan^{-1}\left\{\frac{\beta_{\min}(\phi_d,\phi_s)f(\phi_s)L}{b\Gamma}\right\} \qquad [22]$$

as obtained by equating [4] and [21]. We can also see readily that, for a settler of given dimensions, the global maximum permissible value of $Q_{s,0}$ is reached when $\theta = \theta_{crit}$, in which case

$$Q_{s,0}(\max) = \frac{bu_t Lf(\phi_s)\Gamma}{(1-\phi_s/\phi_d)\sqrt{\{b\Gamma\}^2+\{\beta_{\min}(\phi_d,\phi_s)f(\phi_s)L\}^2}}. \qquad [23]$$

Note that ϕ_d is, strictly speaking, not an independent parameter since, in principle at least, one should be able to extend the analysis by Kapoor & Acrivos (1995) to high aspect ratio vessels and thereby determine the particle concentration profile within the sediment. In that case θ_{crit} would be found to depend only on ϕ_s. The analysis leading to that result, however, has not been attempted thus far.

All the results referred to above pertain to the bottom feeding high aspect ratio settler, where the presence of a large pressure gradient, which opposes the downward flow of the sediment, introduces a constraint on the maximum permissible feed flow rate for continuous operation. In contrast, when the settler is operated in the top feeding mode, a simple analysis, along the lines given earlier, shows that the pressure decreases as one proceeds down the channel, which means that the resulting pressure drop aids rather than hinders the sediment flow. Thus, provided that the angle of inclination exceeds the critical value found earlier by Kapoor & Acrivos (1995) for the flow along an inclined plate of a concentrated sediment in contact with a stagnant sedimenting suspension, the presence of this sediment does not place an additional constraint on the maximum allowable feed rate. In other words, in a settler of effectively infinite length, the expression for $Q_{s0}(\max)$ derived earlier by Davis *et al.* (1983), for the case $\lambda(\phi_s) = 1$,

$$Q_{s,0}(\max) = \frac{bu_t\Gamma\sin\theta}{192} \qquad [24]$$

would be expected to apply with only minor modifications. The above expression is, of course, similar to [21] which applies to the bottom feeding mode. But since, as was shown earlier, $\beta_{\min}$ is $O(10)$, we conclude that, in settling vessels of effectively infinite length, the maximum volumetric feed rate for the bottom feeding mode can exceed that for the top feeding mode by an order of magnitude under otherwise identical conditions.

We conclude by noting that the results presented above are particularly significant in that they provide an improved theoretical basis for the design and optimal performance of supersettlers.

Acknowledgement—This work was supported in part by the U.S. Department of Energy under Grant No. 90ER14139-0006.

REFERENCES

Acrivos, A. & Herbolzheimer, E. 1979 Enhanced sedimentation in settling tanks with inclined walls. *J. Fluid Mech.* **92,** 435–457.

Davis, R. H., Herbolzheimer, E. & Acrivos, A. 1983 Wave formation and growth during sedimentation in narrow tilted channels. *Phys. Fluids* **26,** 2055–2064.

Kapoor, B. & Acrivos, A. 1995 Sedimentation and sediment flow in settling tanks with inclined walls. *J. Fluid Mech.* **290,** 39–66.

Leung, W. F. & Probstein, R. F. 1983 Lamella and tube settlers 1. Model and operation, 2. Flow stability. *Ind. Engng Chem. Proc. Des. Rev.* **22,** 58–67.

Nir, A. & Acrivos, A. 1990 Sedimentation and sediment flow on inclined surfaces. *J. Fluid Mech.* **212,** 139–153.

Probstein, R. F., Yung, R. & Hicks, R. 1981 In *Physical Separations* (Edited by Freeman, M. P. & Fitzpatrick, J. A.), pp. 53–92. Engineering Foundation, New York.

APPENDIX

The solution of [5], [7] and [8] is:

$$u_c = \left(\frac{dP}{dx} - \Gamma \sin\theta\right)\frac{y^2}{2} + c_1 y$$

$$u_s = \frac{1}{\lambda(\phi_s)}\left(\frac{dP}{dx}\frac{y^2}{2} + c_3 y + c_4\right)$$

$$u_d = \frac{1}{\lambda(\phi_d)}\left[\left\{\frac{dP}{dx} + \left(\frac{\phi_d}{\phi_s} - 1\right)\Gamma \sin\theta\right\}\frac{y^2}{2} + c_5 y + c_6\right]$$

$$c_1 = c_3 + \delta\Gamma \sin\theta \quad c_3 = F_1\frac{dP}{dx} + F_2\Gamma \sin\theta$$

$$c_4 = \lambda(\phi_s)\left\{\left(\frac{dP}{dx}\frac{\delta^2}{2} + c_3\delta\right)\left(1 - \frac{1}{\lambda(\phi_s)}\right) + \frac{\delta^2}{2}\Gamma \sin\theta\right\}$$

$$c_5 = c_3 - \xi\left(\frac{\phi_d}{\phi_s} - 1\right)\Gamma \sin\theta$$

$$c_6 = -\frac{1}{2}\left\{\frac{dP}{dx} + \left(\frac{\phi_d}{\phi_s} - 1\right)\Gamma \sin\theta\right\} - c_3 + \xi\left(\frac{\phi_d}{\phi_s} - 1\right)\Gamma \sin\theta$$

$$F_1 = A/D \quad \text{and} \quad F_2 = B/D$$

$$A = -\frac{1}{2}\left[\delta^2\left(1 - \frac{1}{\lambda(\phi_s)}\right) + \xi^2\left(\frac{1}{\lambda(\phi_s)} - \frac{1}{\lambda(\phi_d)}\right) + \frac{1}{\lambda(\phi_d)}\right]$$

$$B = -\frac{1}{2}\left[\frac{(\phi_d/\phi_s - 1)(\xi - 1)^2}{\lambda(\phi_d)} + \delta^2\right]$$

$$D = \delta\left(1 - \frac{1}{\lambda(\phi_s)}\right) + \xi\left(\frac{1}{\lambda(\phi_s)} - \frac{1}{\lambda(\phi_d)}\right) + \frac{1}{\lambda(\phi_d)}$$

$$F_3 = \frac{\delta^3}{6} + F_1\frac{\delta^2}{2}$$

$$F_4 = \frac{\delta^2}{2}(F_2 + \delta) - \frac{\delta^3}{6}$$

$$F_5 = \frac{(\xi^3 - \delta^3)}{6\lambda(\phi_s)} + \frac{F_1(\xi^2 - \delta^2)}{2\lambda(\phi_s)} + \left(1 - \frac{1}{\lambda(\phi_s)}\right)\left(\frac{\delta^2}{2} + \delta F_1\right)(\xi - \delta)$$

$$F_6 = \frac{(\xi^2 - \delta^2)}{2\lambda(\phi_s)}F_2 + \left[\delta\left(1 - \frac{1}{\lambda(\phi_s)}\right)F_2 + \frac{\delta^2}{2}\right](\xi - \delta)$$

$$F_7 = \frac{1}{\lambda(\phi_d)}\left[\frac{(1 - \xi^3)}{6} + \frac{(1 - \xi^2)F_1}{2} - (F_1 + 1/2)(1 - \xi)\right]$$

$$F_8 = \frac{1}{\lambda(\phi_d)}\left[\frac{(1 - \xi^3)(\phi_d/\phi_s - 1)}{6} + \frac{(1 - \xi^2)[F_2 - \xi(\phi_d/\phi_s - 1)]}{2} + [(\xi - 1/2)(\phi_d/\phi_s - 1) - F_2](1 - \xi)\right].$$